A LEVEL SET METHOD FOR THE SEMICLASSICAL LIMIT OF THE SCHRÖDINGER EQUATION WITH DISCONTINUOUS POTENTIALS

DONGMING WEI, SHI JIN, RICHARD TSAI, AND XU YANG

Abstract. We propose a level set method for the semiclassical limit of the Schrödinger equation with discontinuous potentials. A discontinuous potential corresponds to a potential barrier, at which waves can be partially transmitted and reflected. Previously such a problem was handled by Jin and Wen using the Liouville equation–which arises as the semiclassical limit of the Schrödinger equation–with an interface condition to account for partial transmissions and reflections (S. Jin and X. Wen, SIAM J. Num. Anal. 44, 1801-1828, 2006). However, the initial data are Dirac-delta functions which are difficult to approximate numerically with a high accuracy. In this paper, we extend the level set method introduced in (S. Jin, H. Liu, S. Osher and R. Tsai, J. Comp. Phys. 210, 497-518, 2005) for this problem. The advantage of this method is that, via a simple decomposition of the initial data one can evolve in time with *bounded* solution, so as to avoid discretizing the singular delta function numerically until at the output time, thus offering a more accurate numerical approximation.

Two new ideas are introduced here: 1) a decomposition of the problem with *partial* transmission and reflection into the sum of problems with only *complete* transmissions and reflections, so the level set method of Jin-Liu-Osher-Tsai can be used here; 2) a reinitialization technique, which allows us to write the sum of several Dirac-delta functions into one delta function, enabling us to handle multiple transmissions and reflections. We carry out numerical experiments in both one and two space dimensions to verify this new algorithm.

1. Introduction

In this paper, we construct and study a numerical scheme for the Liouville equation in d-dimension:

$$f_t + H_{\mathbf{v}} \cdot \nabla_{\mathbf{x}} f - H_{\mathbf{x}} \cdot \nabla_{\mathbf{v}} f = 0\,, \quad t > 0, \quad \mathbf{x}, \mathbf{v} \in R^d\,, \tag{1.1}$$

where the Hamiltonian H possesses the form

$$H(\mathbf{x}, \mathbf{v}) = \frac{1}{2}|\mathbf{v}|^2 + V(\mathbf{x}) \tag{1.2}$$

with $V(\mathbf{x})$ the potential function. $f(t, \mathbf{x}, \mathbf{v})$ is the density distribution of particles depending on position $\mathbf{x}$, time t and velocity $\mathbf{v}$. We are concerned with the case when $V(\mathbf{x}) \in W^{1,\infty}$ with isolated *discontinuities* due to potential barriers. Waves hitting a potential barrier can undergo partial transmissions and reflections.

The bicharacteristics of the Liouville equation (1.1) satisfy the Hamiltonian system:

$$\frac{d\mathbf{x}}{dt} = \mathbf{v}\,, \quad \frac{d\mathbf{v}}{dt} = -\nabla_{\mathbf{x}} V(\mathbf{x})\,. \tag{1.3}$$

In classical mechanics the Hamiltonian (1.2) of a particle remains a constant along the particle trajectory, even when it is being transmitted or reflected by the interface.

This Liouville equation arises in the phase space description of the semiclassical limit [7, 21] of the Schödinger equation:

$$i\hbar\partial_t \psi^\hbar = -\frac{\hbar^2}{2}\Delta\psi^\hbar + V(x)\psi^\hbar, \qquad x \in \mathbb{R}^n, \tag{1.4}$$

Date: November 5, 2009.

where $\psi^\hbar$ is the complex-valued wave function, $\hbar$ the reduced Planck constant. The Liouville equation has been the basis of many recent numerical methods for high frequency waves or the semiclassical limit of the Schödinger equation, see [2, 3, 5, 6, 9, 14, 23], when the potential function V is smooth. At the discontunuities of V, the semiclassical limit has to account for partial transmissions and reflections [1, 22, 25]. In the works of Jin and Wen [15, 17], the interface transmissions and reflections are formulated as interface conditions that are used to couple the Liouville equation (1.1) away from the interfaces, and then the interface conditions are built into the numerical fluxes for the Liouville equation, resulting in a class of numerical methods for high frequency waves through interfaces that can capture partial transmissios and reflections *without* numerically resolving the short wave length. Such a method has been extended for quantum barriers [11, 12, 13] and for wave diffractions [18, 19].

One of the difficulties in using the Liouville equation is the singular initial data. Indeed, if one considers the Schrödinger equation (1.4) with the WKB initial data

$$\psi(x,0) = A_0(x)\exp(iS_0(x)/\epsilon)\,, \tag{1.5}$$

one arrives, in the semiclassical limit $\hbar \to 0$, the following mono-kinetic initial data for the Liouville equation (1.1):

$$f(0,\mathbf{x},\mathbf{v}) = |A_0(\mathbf{x})|^2\delta(\mathbf{v} - \nabla_{\mathbf{x}}S_0(\mathbf{x})) \tag{1.6}$$

Even for a smooth potential, the solution to (1.1) and (1.6) are sum of Dirac-delta functions correponding to multivalued velocity and density [8, 26]. Numerical solutions of such singular solutions are usually poor, since one needs to first approximate the delta function in (1.6) initially and then evolve such data in time by solving the Liouville equation (1.1) (hereafter called the *direct method*) with numerical schemes that typically introduce numerical dissipation. An improved method (hereafter called the *decomposition method*) was introduced in [9], where f was decomposed into ϕ and ψ_i $(i = 1, \cdots, d)$ where ϕ and ψ_i solve the same Liouville equation (1.1) with initial data

$$\phi(\mathbf{x},\mathbf{v},0) = \rho_0(\mathbf{x})\,, \quad \psi_i(\mathbf{x},\mathbf{v},0) = v_i - u_{i0}(\mathbf{x})\,, \tag{1.7}$$

respectively. This allows the numerical computations for a bounded solution rather than measure-valued solution of the Liouville equation with singular initial data (1.6), which greatly enhances the numerical accuracy. The moments (such as the density ρ and momentum $\rho\mathbf{u}$ can be recovered through

$$\rho(\mathbf{x},t) = \int \phi(\mathbf{x},\mathbf{v},t)\Pi_{i=1}^d\delta(\psi_i)d\mathbf{v}, \tag{1.8}$$

$$\mathbf{u}(\mathbf{x},t) = \int \phi(\mathbf{x},\mathbf{v},t)\mathbf{v}\Pi_{i=1}^d\delta(\psi_i)d\mathbf{v}/\rho(\mathbf{x},t)\,. \tag{1.9}$$

Numerical results in [9] showed an improved numerical accuracy and resolution of this decomposition method than the direct method. This decomposition method can be extended to potential barriers with *complete* transmissions and reflections [15, 16]. But for partial transmissions and reflections, extra level set functions are needed each time the particle hits the interface and then splits into a reflected one and a transmitted one, thus the total number of level set functions will increase exponentially in time with multiple transmissions and reflections [2, 17].

The goal of this paper is to extend the decomposition method for partial transmissions and reflections. In order to achieve this, we introduce two new ideas here. First, we decompose the problem with *partial* transmission and reflection into the sum of problems with only *complete* transmissions and reflections, so the decomposition method of Jin-Liu-Osher-Tsai can be used here as in [15, 16]. Secondly, a reinitialization technique, which allows us to write the sum of several Dirac-delta functions into one delta function, is introduced. This enables us to handle multiple transmissions and reflections. We carry out numerical experiments to verify the proposed new algorithm.

We give the details of decomposition in section 2. In section 3, we state the level set formulation of the corresponding systems. In section 4, we give details of how we do the reinitialization. In section 5, we give some numerical examples. At last, we make some concluding remarks.

2. Decomposition of the interface problem

We illustrate our idea in the following simple 1D example. The result can be extended to any space dimension and any geometry without difficulty.

Assuming the interface is at $x = 0$ with $V_r - V_l = \Delta V$, we consider the following initial value problem with interface conditions

$$\begin{cases} \mathcal{L}f = \partial_t f + \xi f_x - V_x f_\xi = 0, \\ f(0,x,\xi) = f_0(x,\xi) \\ f(t,0^+,\xi^+) = R(\xi^+) f(t,0^+,-\xi^+) + T(\xi^-) f(t,0^-,\xi^-), \quad \xi^+ \geq 0 \\ f(t,0^-,\xi^-) = R(\xi^-) f(t,0^-,-\xi^-) + T(\xi^+) f(t,0^+,\xi^+), \quad \xi^- \leq 0 \end{cases} \tag{2.1}$$

Here $\mathcal{L}$ is the linear Liouville operator defined by

$$\mathcal{L} := \partial_t + \xi \partial_x - V_x \partial_\xi \,, \tag{2.2}$$

ξ^+ and ξ^-, having the same sign, satisfy the conservation of Hamiltonian

$$(\xi^-)^2 + V_l = (\xi^+)^2 + V_r \,. \tag{2.3}$$

Note that the solution to the Liouville equation (1.1) cannot be suitably defined at the discontinuities of V. With the interface condition in (2.1), the problem becomes well-posed [17]. In particular, the solution to (2.1) can be solved by a method of (generalized) characteristics. Let $\Omega_1(t)$ denote all (x,ξ) such that they can be traced backward along the trajectory of the Hamiltonian system (1.3) to $t = 0$ without hitting the interface $x = 0$, while $\Omega_2(t)$ consists of all other (x,ξ), i.e., if we trace (x,ξ) backward along the the trajectory of (1.3), it hits the interface at some time t_c. The solution to (2.1) is then given by (assuming that the backward trajectory of (1.3) hits $x = 0$ at most once):

- If $(x(t),\xi(t)) \in \Omega_1$, then

$$f(t,x,\xi) = f_0(x_0,\xi_0) \,, \tag{2.4}$$

  where (x_0,ξ_0) is the solution of (1.3) backward in time at $t = 0$ with initial data $(x(t),\xi(t))$ at time t.
- If $(x(t),\xi(t)) \in \Omega_2$, then

$$\begin{aligned} f(t,x,\xi) &= R(\xi^+) f(t_c,0^+,-\xi^+) + T(\xi^-) f(t_c,0^-,\xi^-). \\ &= R(\xi^+) f_0(x_0^R,\xi_0^R) + T(\xi^-) f_0(x_0^T,\xi_0^T). \end{aligned} \tag{2.5}$$

  See Figure 1.

We now show that the solution to (2.1), as defined above, can be written as the sum of three interface problems satisfied by the same Liouville equation, but with *complete* transmissions and reflection. The result is stated in the following theorem.

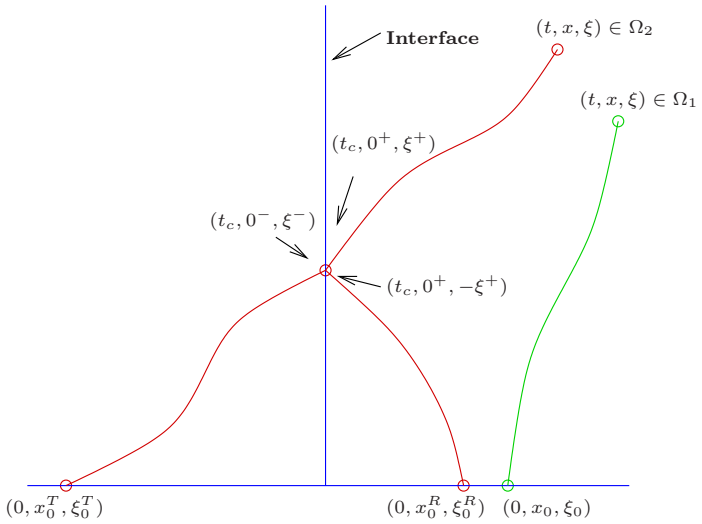

Figure 1: Illustration of the characteristic solution.

Theorem 2.1. *Let f be the generalized characteristic solution of (2.1). Consider the following three initial value problems with interface conditions:*

$$\begin{cases} \mathcal{L}f^R = 0, \quad f^R(0,x,\xi) = f_0^R(x,\xi) := f_0(x,\xi) \\ f^R(t,0^+,\xi^+) = R(\xi^+)f^R(t,0^+,-\xi^+), \quad \xi^+ \geq 0 \\ f^R(t,0^-,\xi^-) = R(\xi^-)f^R(t,0^-,-\xi^-), \quad \xi^- \leq 0 \end{cases} \tag{2.6}$$

$$\begin{cases} \mathcal{L}f^{T1} = 0, \quad f^{T1}(0,x,\xi) = f_0^{T1}(x,\xi) := I_{\{x<0\}}f_0(x,\xi) \\ f^{T1}(t,0^+,\xi^+) = T(\xi^-)f^{T1}(t,0^-,\xi^-), \quad \xi^+ \geq 0 \\ f^{T1}(t,0^-,\xi^-) = T(\xi^+)f^{T1}(t,0^+,\xi^+), \quad \xi^- \leq 0 \end{cases} \tag{2.7}$$

and

$$\begin{cases} \mathcal{L}f^{T2} = 2, \quad f^{T2}(0,x,\xi) = f_0^{T2}(x,\xi) := I_{\{x\geq 0\}}f_0(x,\xi) \\ f^{T2}(t,0^+,\xi^+) = T(\xi^-)f^{T2}(t,0^-,\xi^-), \quad \xi^+ \geq 0 \\ f^{T2}(t,0^-,\xi^-) = T(\xi^+)f^{T1}(t,0^+,\xi^+), \quad \xi^- \leq 0 \end{cases} \tag{2.8}$$

where ξ^+ and ξ^- satisfy condition (2.3) with the same sign. If no characteristic hits the interface $x = 0$ more than once for $0 \leq t \leq K$, then

$$f = f^R + I_{\{x\geq 0\}}f^{T1} + I_{\{x<0\}}f^{T2}, \quad 0 \leq t \leq K. \tag{2.9}$$

Proof. Let $0 \leq t \leq K$. We decompose the x-ξ plane into two parts: $\Omega_1(t)$ and $\Omega_2(t)$. According to the definition of the solution to (2.1),

$$f(t,x,\xi) = I_{\Omega_1}f_0(x_0,\xi_0) + I_{\Omega_2}R(\xi^+)f_0(x_0^R,\xi_0^R) + I_{\Omega_2}T(\xi^-)f_0(x_0^T,\xi_0^T). \tag{2.10}$$

Similarly,

$$f^R(t,x,\xi) = I_{\Omega_1} f_0(x_0,\xi_0) + I_{\Omega_2} R(\xi^+) f_0(x_0^R,\xi_0^R), \tag{2.11}$$

$$f^{T1}(t,x,\xi) = I_{\Omega_1} I_{\{x_0<0\}} f_0(x_0,\xi_0) + I_{\Omega_2} T(\xi^-) I_{\{x_0^T<0\}} f_0(x_0^T,\xi_0^T), \tag{2.12}$$

$$f^{T2}(t,x,\xi) = I_{\Omega_1} I_{\{x_0\geq 0\}} f_0(x_0,\xi_0) + I_{\Omega_2} T(\xi^-) I_{\{x_0^T\geq 0\}} f_0(x_0^T,\xi_0^T), \tag{2.13}$$

By the definitions of Ω_1, for all $(x,\xi)\in\Omega_1$, one can trace backward in time along the trajectory of (1.3) to (x_0,ξ_0) without hitting the interface $x=0$. Therefore, $x_0<0$ if and only if $x<0$. Thus

$$I_{\Omega_1} I_{\{x_0<0\}} = I_{\Omega_1 \bigcap \{x<0\}}, \qquad I_{\Omega_1} I_{\{x_0\geq 0\}} = I_{\Omega_1 \bigcap \{x\geq 0\}}.$$

Similarly, definitions of Ω_2 and x_0^T imply that

$$I_{\Omega_2} I_{\{x_0^T<0\}} = I_{\Omega_2 \bigcap \{x\geq 0\}}, \qquad I_{\Omega_2} I_{\{x_0^T\geq 0\}} = I_{\Omega_2 \bigcap \{x<0\}}.$$

Hence

$$\begin{aligned}
& f^R(t,x,\xi) + I_{\{x\geq 0\}} f^{T1}(t,x,\xi) + I_{\{x<0\}} f^{T2}(t,x,\xi) \\
= \; & I_{\Omega_1} f_0(x_0,\xi_0) + I_{\Omega_2} R(\xi^+) f_0(x_0^R,\xi_0^R) + \\
& I_{\{x\geq 0\}} I_{\Omega_1 \bigcap \{x<0\}} f_0(x_0,\xi_0) + I_{\{x\geq 0\}} I_{\Omega_2 \bigcap \{x\geq 0\}} T(\xi^-) f_0(x_0^T,\xi_0^T) + \\
& I_{\{x<0\}} I_{\Omega_1 \bigcap \{x\geq 0\}} f_0(x_0,\xi_0) + I_{\{x<0\}} I_{\Omega_2 \bigcap \{x<0\}} T(\xi^-) f_0(x_0^T,\xi_0^T) \\
= \; & I_{\Omega_1} f_0(x_0,\xi_0) + I_{\Omega_2} R(\xi^+) f_0(x_0^R,\xi_0^R) + I_{\Omega_2} T(\xi^-) f_0(x_0^T,\xi_0^T) \\
= \; & f(t,x,\xi).
\end{aligned}$$

□

Theorem 2.1 shows that an interface problem with partial transmissions and reflections can be written as sum of interface problems with complete transmissions and reflections, as long as the particle trajectory does not hit the interface more than once. Based on this result, we can use the following strategy to obtain the solution of (2.1): for $0\leq t\leq K$, we solve problems (2.6), (2.7) and (2.8), then

$$f(t,x,\xi) = f^R(t,x,\xi) + f^{T1}(t,x,\xi) + f^{T2}(t,x,\xi), \quad 0\leq t\leq K\,.$$

Using $f(K,x,\xi)$ as the initial data, we redo the previous step to get solution of (2.1) on $[K,2K]$. One can repeat this process to obtain the solution for any time interval $[0,T]$.

Remark 2.1. *If all the characteristics hit the interface with $|\xi^+|>C>0$ and $|\xi^-|>C>0$, where C is a positive constant, then we can always find a constant K, such that no characteristic will hit the interface more than once in any time period with length K. Hence following the above strategy gives us the exact solution of (2.1).*

Remark 2.2. *If there is no K can grantee that every characteristic hits the interface at most once in any time period with length K, we can still perform our strategy to get a solution. And the difference between our solution and the exact solution is bounded by a function of K (which goes to 0 as K goes to 0), no matter how many steps were performed. We explain the details below.*

For a chosen K, we can find $C>0$, such that if $|\xi^+|>C$ and $|\xi^-|>C$, then the characteristic will not hit the interface more than once in any time period with length K. So no matter how many steps were performed, the solution for this part is exact. The remaining part, which corresponds to $|\xi^\pm|\leq C(K)$, goes to 0 as K goes to 0.

Remark 2.3. *If there are N interfaces which divide $\mathbb{R}^1$ into $N+1$ parts denoted by $A_1, A_2, \ldots, A_{N+1}$ respectively, then the solution f will be*

$$f = f^R + \sum_{i=1}^{N+1} I_{\{\mathbb{R}^1 \setminus A_i\}} f^{T_i},$$

where each f^{T_i} has the initial data

$$f^{T_i}(0, x, \xi) = f_0^{T_i}(x, \xi) := I_{A_i} f_0(x, \xi).$$

Similarly, in the multi-dimensional case, if the interfaces divide $\mathbb{R}^n$ into $N+1$ parts denoted by $A_1, A_2, \ldots, A_{N+1}$ respectively, then the solution f will be

$$f = f^R + \sum_{i=1}^{N+1} I_{\{\mathbb{R}^n \setminus A_i\}} f^{T_i},$$

where each f^{T_i} has the initial data

$$f^{T_i}(0, x, \xi) = f_0^{T_i}(x, \xi) := I_{A_i} f_0(x, \xi).$$

3. The level set decomposition

Consider the δ function initial data (1.6), namely,

$$f(0, x, \xi) = f_0(x, \xi) = \rho_0(x)\delta\big(\xi - u_0(x)\big). \tag{3.1}$$

Correspondingly, the initial data for f^R, f^T and f^R, which only involve complete transmission or reflection, are of the mono-kinetic form (3.1). According to [15, 16], they can be solved by the decomposition method of [9]. More specifically, $f^R = \psi^R \delta(\phi^R)$ where ϕ^R and ψ^R satisfy

$$\begin{cases} \mathcal{L}\phi^R = 0, \quad \phi_0^R(x) = \xi - u_0(x) \\ \phi^R(t, 0^+, \xi^+) = \phi^R(t, 0^+, -\xi^+), \quad \xi^+ \geq 0 \\ \phi^R(t, 0^-, \xi^-) = \phi^R(t, 0^-, -\xi^-), \quad \xi^- \leq 0 \end{cases} \tag{3.2}$$

$$\begin{cases} \mathcal{L}\psi^R = 0, \quad \psi_0^R(x) = \rho_0(x) \\ \psi^R(t, 0^+, \xi^+) = R(\xi^+)\psi^R(t, 0^+, -\xi^+), \quad \xi^+ \geq 0 \\ \psi^R(t, 0^-, \xi^-) = R(\xi^-)\psi^R(t, 0^-, -\xi^-), \quad \xi^- \leq 0 \end{cases} \tag{3.3}$$

Similarly, $f^{T1} = \psi^{T1}\delta(\psi^{T1})$ and $f^{T2} = \psi^{T2}\delta(\psi^{T2})$ where

$$\begin{cases} \mathcal{L}\phi^{T1} = 0, \quad \phi_0^{T1}(x) = \xi - u_0(x) \\ \phi^{T1}(t, 0^+, \xi^+) = \phi^{T1}(t, 0^-, \xi^-), \quad \xi^+ \geq 0 \\ \phi^{T1}(t, 0^-, \xi^-) = \phi^{T1}(t, 0^+, \xi^+), \quad \xi^- \leq 0 \end{cases} \tag{3.4}$$

$$\begin{cases} \mathcal{L}\psi^{T1} = 0, \quad \psi_0^{T1}(x) = I_{\{x<0\}}\rho_0(x) \\ \psi^{T1}(t,0^+,\xi^+) = T(\xi^+)\psi^{T1}(t,0^-,\xi^-), \quad \xi^+ \geq 0 \\ \psi^{T1}(t,0^-,\xi^-) = T(\xi^-)\psi^{T1}(t,0^+,\xi^+), \quad \xi^- \leq 0 \end{cases} \tag{3.5}$$

$$\begin{cases} \mathcal{L}\phi^{T2} = 0, \quad \phi_0^{T2}(x) = \xi - u_0(x) \\ \phi^{T2}(t,0^+,\xi^+) = \phi^{T2}(t,0^-,\xi^-), \quad \xi^+ \geq 0 \\ \phi^{T2}(t,0^-,\xi^-) = \phi^{T2}(t,0^+,\xi^+), \quad \xi^- \leq 0 \end{cases} \tag{3.6}$$

$$\begin{cases} \mathcal{L}\psi^{T2} = 0, \quad \psi_0^{T2}(x) = I_{\{x\geq 0\}}\rho_0(x) \\ \psi^{T2}(t,0^+,\xi^+) = T(\xi^+)\psi^{T2}(t,0^-,\xi^-), \quad \xi^+ \geq 0 \\ \psi^{T2}(t,0^-,\xi^-) = T(\xi^-)\psi^{T2}(t,0^+,\xi^+), \quad \xi^- \leq 0 \end{cases} \tag{3.7}$$

At time K, one can sum these solutions to obtain

$$f(K) = f^R + f^{T1} + f^{T2} = \psi^R\delta(\phi^R) + \psi^{T1}\delta(\phi^{T1}) + \psi^{T2}\delta(\phi^{T2}) \tag{3.8}$$

4. Reinitialization

As discussed in the previous section, even though f_0 is monokinetic (3.1), at time K it is a sum of more than one delta-functions. In fact, it may be the sum of more than three delta-functions shown in (3.8), since ϕ^{R,T_1,T_2} may have multiple zeroes, corresponding to multiphased velocities [8, 26]. Clearly, to continue the decomposition of section 3, we need to reinitialize $f(K,x,\xi)$ so it becomes mono-kinetic data like (3.1). In other words, we want to find ϕ and ψ such that

$$\begin{aligned} & f(x,\xi,K) \\ = \ & \psi^R(x,\xi,K)\delta\Big(\phi^R(x,\xi,K)\Big) + \psi^{T1}(x,\xi,K)\delta\Big(\phi^{T1}(x,\xi,K)\Big) + \psi^{T2}(x,\xi,K)\delta\Big(\phi^{T2}(x,\xi,K)\Big) \\ = \ & \psi(x,\xi,K)\delta\Big(\phi(x,\xi,K)\Big). \end{aligned} \tag{4.1}$$

The following theorems provide a generic stragety on how this can be done.

Theorem 4.1. *(1-Dimension) Assume $g_j(x)$ are continuous functions with N_j distinct zeros x_{j_i}, $i = 1,\cdots,N_j$, $j = 1,\cdots,N$. Assume $f_j(x)$ are bounded continuous functions. Then there exists an $\epsilon > 0$ and a function κ defined by*

$$\kappa(x) = \begin{cases} 1, & |x| < \epsilon \\ 0, & |x| \geq \epsilon \end{cases} \tag{4.2}$$

such that

$$\sum_{j=1}^{N} f_j(x)\delta\Big(g_j(x)\Big) = f(x)\delta\Big(g(x)\Big) \tag{4.3}$$

in the distributional sense. Here

$$f(x) = \sum_{j=1}^{N} f_j(x)\kappa\Big(g_j(x)\Big)\,, \tag{4.4}$$

and $g(x)$ is defined by

$$g(x) = sgn\Big(g_{k_x}(x)\Big)\min_j\Big(\big|g_j(x)\big|\Big), \tag{4.5}$$

where k_x is the index such that $\Big|g_{k_x}(x)\Big| \le \Big|g_j(x)\Big|$, $\forall\, j$.

Proof. Since $g_j(x)$ are continuous with distinct zeros, there exists an $\eta > 0$ small enough, such that

$$(x_{j_i} - \eta, x_{j_i} + \eta), \quad i = 1, \cdots, N_j, \quad j = 1, \cdots, N$$

are disjoint intervals and

$$\max_{1\le j\le N, 1\le i\le N_j}\left(\max_{x\in(x_{j_i}-\eta, x_{j_i}+\eta)}\Big|g_j(x)\Big|\right) < \min_{1\le j\le N, 1\le i\le N_j}\left(\min_{x\in(x_{j_i}-\eta, x_{j_i}+\eta), m\ne j}\Big|g_m(x)\Big|\right),$$

Let

$$\epsilon = \max_{1\le j\le N, 1\le i\le N_j}\left(\max_{x\in(x_{j_i}-\eta, x_{j_i}+\eta)}\Big(\big|g_j(x)\big|\Big)\right), \tag{4.6}$$

then on each interval $(x_{j_i} - \eta, x_{j_i} + \eta)$,

$$f(x) = f_j(x)$$

and

$$g(x) = g_j(x).$$

Furthermore, one can find a positive number θ, such that

$$g(x) > \theta > 0, \quad \forall\, x \in \mathbb{R}\Big\backslash \bigcup_{1\le j\le N, 1\le i\le N_j}(x_{j_i} - \eta, x_{j_i} + \eta). \tag{4.7}$$

Therefore, $\forall\, \varphi \in C_c^\infty(\mathbb{R})$,

$$\int_{-\infty}^{\infty}\varphi(x)f(x)\delta\Big(g(x)\Big)dx = \sum_{j=1}^{N}\sum_{i=1}^{N_j}\int_{x_{j_i}-\eta}^{x_{j_i}+\eta}\varphi(x)f(x)\delta\Big(g(x)\Big)dx\,. \tag{4.8}$$

Hence, for all test functions $\varphi \in C_c^\infty(\mathbb{R})$,

$$\begin{aligned} & \int_{-\infty}^{\infty} \varphi(x) \sum_{j=1}^{N} f_j(x)\delta\Big(g_j(x)\Big)dx \\ = & \sum_{j=1}^{N} \int \varphi(x) f_j(x)\delta\Big(g_j(x)\Big)dx \\ = & \sum_{j=1}^{N}\sum_{i=1}^{N_j} \int_{x_{j_i}-\eta}^{x_{j_i}+\eta} \varphi(x) f_j(x)\delta\Big(g_j(x)\Big)dx \\ = & \sum_{j=1}^{N}\sum_{i=1}^{N_j} \int_{x_{j_i}-\eta}^{x_{j_i}+\eta} \varphi(x) f(x)\delta\Big(g(x)\Big)dx \\ = & \int_{-\infty}^{\infty} \varphi(x) f(x)\delta\Big(g(x)\Big)dx. \end{aligned} \tag{4.9}$$

This completes the proof. □

Theorem 4.2. *(Multi-Dimension) Assume $g_j(x)$ are C^1 continuous functions such that $\int_{\mathbb{R}^n} \delta\Big(g_j(x)\Big)dx < \infty$ for $j = 1, \cdots, N$. Denote the zeros sets of $g_j(x)$ by Ω_j. Assume that $M\Big(\Omega_{j_1} \cap \Omega_{j_2}\Big) = 0$, $\forall\, j_1, j_2$. Suppose there exists a constant $C > 0$ such that*

$$\Big|Dg_j(x)\Big| > C, \quad \forall\, j \quad \forall\, x \in \Omega_j. \tag{4.10}$$

Let $f_j(x)$ be bounded continuous functions. Define the function κ_ϵ by

$$\kappa_\epsilon(x) = \begin{cases} 1, & |x| < \epsilon \\ 0, & |x| \geq \epsilon\,. \end{cases} \tag{4.11}$$

Then

$$f_\epsilon(x)\delta\Big(g(x)\Big) \rightharpoonup \sum_{j=1}^{N} f_j(x)\delta\Big(g_j(x)\Big), \quad \epsilon \to 0 \tag{4.12}$$

in the distributional sense. Here

$$f_\epsilon(x) = \sum_{j=1}^{N} f_j(x)\kappa_\epsilon\Big(g_j(x)\Big)\,, \tag{4.13}$$

and $g(x)$ is defined by

$$g(x) = g_{k_x}(x) \tag{4.14}$$

where k_x is the index such that $\Big|g_{k_x}(x)\Big| \leq \Big|g_j(x)\Big|$, $\forall\, j$.

Proof. For every fixed test function $\varphi(x) \in C_c^\infty(\mathbb{R}^n)$, for every fixed $\eta > 0$, one can choose θ small enough such that

$$\left| \int_{\mathbb{R}^n} \varphi(x) \sum_{j=1}^{N} f_j(x)\delta\Big(g_j(x)\Big)dx - \sum_{j=1}^{N} \int_{\Omega_j^\theta} \varphi(x) f_j(x)\delta\Big(g_j(x)\Big)dx \right| < \frac{1}{2}\eta, \tag{4.15}$$

where Ω_j^θ is a subset of Ω_j with $M(\Omega_j^\theta) < \infty$ and $\text{dist}(\Omega_{j_1}, \Omega_{j_2}) > C_1 > 0$, $\forall\, j_1,\, j_2$. Following the same idea of the proof of Theorem 4.1, one can further choose a $\varrho > 0$ small enough, such that if $0 < \epsilon < \varrho$ then

$$\sum_{j=1}^{N} \int_{\Omega_j^\theta} \varphi(x) f_j(x) \delta\Big(g_j(x)\Big) dx = \int_{\bigcup \Omega_j^\theta} \varphi(x) f_\epsilon(x) \delta\Big(g(x)\Big) dx. \tag{4.16}$$

We chose $\theta > 0$ small enough so that

$$\int_{\mathbb{R}^n \setminus \bigcup \Omega_j^\theta} \varphi(x) \Big(\sum_{j=1}^{N} |f_j(x)| \Big) \delta\Big(g(x)\Big) dx < \frac{1}{2}\eta. \tag{4.17}$$

Combining (4.15), (4.16) and (4.17), we obtain that for every fixed $\varphi(x) \in C_c^\infty(\mathbb{R}^n)$, and for every fixed $\eta > 0$, there exists $\varrho > 0$, such that if $0 < \epsilon < \varrho$, then

$$\left| \int_{\mathbb{R}^n} \varphi(x) \sum_{j=1}^{N} f_j(x) \delta\Big(g_j(x)\Big) dx - \int_{\mathbb{R}^n} \varphi(x) f_\epsilon(x) \delta\Big(g(x)\Big) dx \right| < \eta. \tag{4.18}$$

□

Corollary 4.1. *If $n \geq 2$ and $g_j(x)$ are piecewise C^1 continuous functions, then the conclusion of Theorem 4.2 is still true.*

5. Numerical examples

In this section, we give several numerical examples. In each example, we compute the density and momentum which are given by

$$\rho = \int f(t, x, \xi) d\xi,$$

$$\rho u = \int \xi f(t, x, \xi) d\xi.$$

We use the upwind scheme to compute all the one-dimensional examples with a minmod slope limiter and the two-dimensional example with no slope limiter.

When computing the physical observables, we use the following discretized delta function [4],

$$\delta_b(x) = \begin{cases} \frac{1}{2b}(1 + \cos\frac{|\pi x|}{b}), & \left|\frac{x}{b}\right| \leq 1, \\ 0, & \text{otherwise}, \end{cases} \tag{5.1}$$

where the parameter b is taken as $b = 0.5\sqrt{\Delta x}$.

Example 5.1. *(Plane waves) We consider (2.1) with the following parameters:*

$$V = \begin{cases} 0 & x \leq 0, \\ 0.045 & x > 0. \end{cases} \qquad R = 0.2, \quad T = 0.8,$$

and the initial conditions:

$$\rho_0(x) = I_{\{x \leq 0\}}, \qquad u_0(x) = 0.5.$$

dx	0.02	0.01	0.005
$\|\rho_{err}\|_1$	1.20×10^{-1}	8.06×10^{-2}	5.07×10^{-2}
$\|(\rho u)_{err}\|_1$	5.51×10^{-2}	3.60×10^{-2}	2.15×10^{-2}

TABLE 1. Example 5.1, the l^1 errors of the density and momentum.

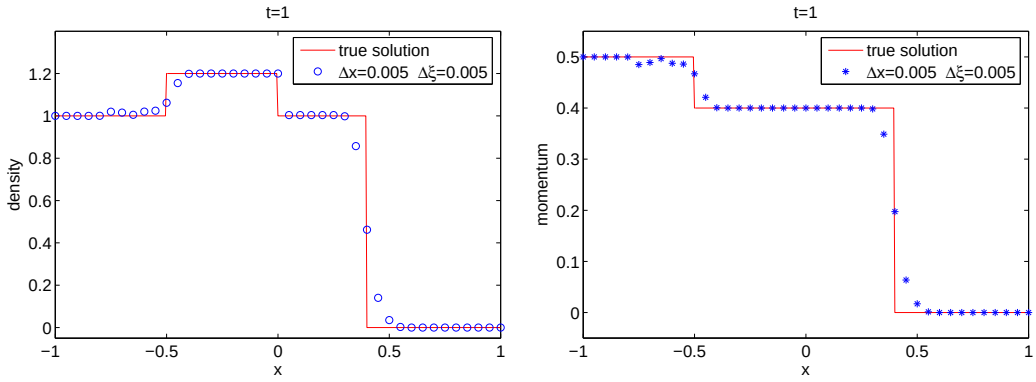

Figure 1: Example 5.1, the comparison of density and momentum between the analytical solution and numerical solution.

One could solve this problem analytically, and the solution at the time $t = 1$ is

$$\begin{aligned} f(t,x,\xi) &= I_{\{x\le 0\}}\delta(\xi-0.5)+0.2I_{\{-0.5\le x\le 0\}}\delta(\xi+0.5)+0.8I_{\{0\le x\le 0.4\}}\delta(\sqrt{\xi^2+0.09}-0.5) \\ &= I_{\{x\le 0\}}\delta(\xi-0.5)+0.2I_{\{-0.5\le x\le 0\}}\delta(\xi+0.5)+I_{\{0\le x\le 0.4\}}\delta(\xi-0.4). \end{aligned}$$

The analytical density and momentum are given by

$$\rho = \begin{cases} 1 & x \le -0.5, \\ 1.2 & -0.5 < x \le 0, \\ 1 & 0 < x \le 0.4, \\ 0 & 0.4 < x. \end{cases} \qquad \rho u = \begin{cases} 0.5 & x \le -0.5, \\ 0.4 & -0.5 < x \le 0, \\ 0.4 & 0 < x \le 0.4, \\ 0 & 0.4 < x. \end{cases}$$

The errors and comparison figures are given in Table 1 and Figure 1. The convergence orders for the density and momentum are 0.6215 and 0.6775.

Example 5.2. *(Harmonic oscillator) We consider (2.1) with the following parameters:*

$$V = \begin{cases} x^2/20 & x \le 0, \\ x^2/20 + 0.045 & x > 0. \end{cases} \qquad R = 0.2, \quad T = 0.8,$$

and the initial conditions:

$$\rho_0(x) = \exp(-100(x+0.3)^2), \qquad u_0(x) = 0.5.$$

The reference solution is computed in fine mesh and using small time steps. The comparison is given in Figure 2.

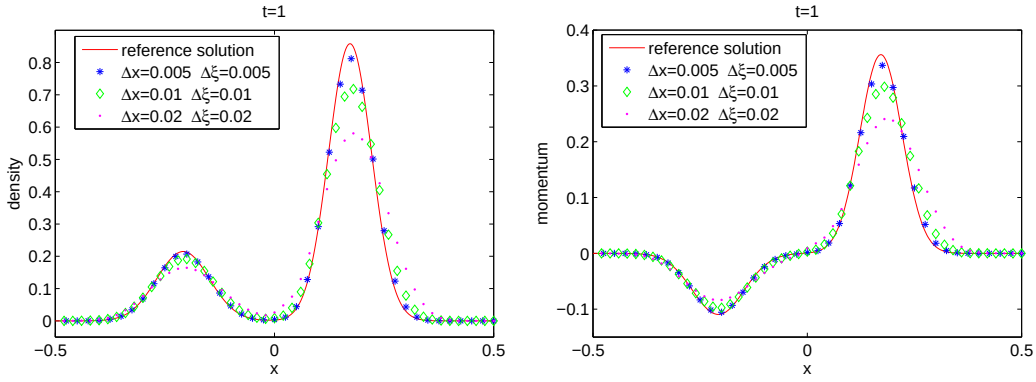

Figure 2: Example 5.2, the comparison of density and momentum between the reference solution and numerical solution.

Example 5.3. *(Reinitialization) We consider (2.1) with the following parameters:*

$$V = \begin{cases} 0 & x \le 0, \\ 2x^2 + 0.045 & x > 0. \end{cases} \qquad R = 0.2, \quad T = 0.8,$$

and the initial conditions:

$$\rho_0(x) = I_{\{x\le 0\}}, \qquad u_0(x) = 0.5.$$

In this example, the particles will hit the interface frequently due to the strong harmonic potential in the domain $\{x > 0\}$. We assume the speed of the particle becomes zero at $x = x_{turn}$, then by the conservation of Hamiltonian,

$$\frac{0.5^2}{2} = 0.045 + \frac{(\xi^+)^2}{2} = 0.045 + 4x_{turn}^2,$$

one has $\xi^+ = 0.4$, $x_{turn} = 0.2$ which implies a lower bound for the reinitialization time is $K = 1$ (actually the second hitting time is $t = \pi/2$).

We compare the numerical solution with analytical solution at $t = 1$ and $t = 2$. When reinitialization, we let κ be the following cutoff function

$$\kappa(x) = \begin{cases} 1, & |x| \le 0.5\sqrt{dx} \\ 0, & |x| > 0.5\sqrt{dx} \end{cases}$$

Following [27], one can find the analytical solution. The analytical solution at $t = 1$ is given by (5.2)

$$\begin{aligned} f(t,x,\xi) \;=\; & I_{\{x\le 0\}}\delta(\xi - 0.5) + 0.2I_{\{-0.5\le x\le 0\}}\delta(\xi + 0.5) + 0.8I_{\{0\le x\le 0.2\}}\frac{1}{0.8\sqrt{1-25x^2}}\delta\Big(\xi - 0.4\sqrt{1-25x^2}\Big) \\ & + 0.8I_{\{0.2\sin 2\le x<0.2\}}\frac{1}{0.8\sqrt{1-25x^2}}\delta\Big(\xi + 0.4\sqrt{1-25x^2}\Big) \end{aligned}$$

The analytical density and momentum at $t = 1$ are given by

$$\rho = \begin{cases} 1 & x \le -0.5, \\ 1.2 & -0.5 < x \le 0, \\ \dfrac{1}{\sqrt{1-25x^2}} & 0 < x \le 0.2\sin 2, \\ \dfrac{2}{\sqrt{1-25x^2}} & 0.2\sin 2 < x \le 0.2, \\ 0 & x > 0.2. \end{cases} \qquad \rho u = \begin{cases} 0.5 & x \le -0.5, \\ 0.4 & -0.5 < x \le 0, \\ 0.4 & 0 < x \le 0.2\sin 2, \\ 0 & 0.2\sin 2 < x. \end{cases}$$

The analytical solution at $t = 2$ is given by

$$\begin{aligned} f(t,x,\xi) &= I_{\{x\le 0\}}\delta(\xi-0.5) + 0.2I_{\{-1\le x\le 0\}}\delta(\xi+0.5) + 0.64I_{\{\pi/4-1\le x<0\}}\delta(\xi+0.5) \\ &\quad +0.8I_{\{0\le x\le 0.2\}}\frac{1}{0.8\sqrt{1-25x^2}}\delta\Big(\xi-0.4\sqrt{1-25x^2}\Big) \\ &\quad +0.8I_{\{0\le x<0.2\}}\frac{1}{0.8\sqrt{1-25x^2}}\delta\Big(\xi+0.4\sqrt{1-25x^2}\Big) \\ &\quad +0.16I_{\{0\le x\le 0.2\sin 2(2-\pi/2)\}}\frac{1}{0.8\sqrt{1-25x^2}}\delta\Big(\xi-0.4\sqrt{1-25x^2}\Big) \end{aligned} \tag{5.3}$$

The analytical density and momentum at $t = 2$ are given by

$$\rho = \begin{cases} 1 & x \le -1, \\ 1.2 & -1 < x \le \pi/4-1, \\ 1.84 & \pi/4-1 < x \le 0, \\ \dfrac{2.2}{\sqrt{1-25x^2}} & 0 < x \le 0.2\sin 2(2-\pi/2), \\ \dfrac{2}{\sqrt{1-25x^2}} & 0.2\sin 2(2-\pi/2) < x \le 0.2, \\ 0 & x > 0.2. \end{cases} \qquad \rho u = \begin{cases} 0.5 & x \le -1, \\ 0.4 & -1 < x \le \pi/4-1, \\ 0.08 & \pi/4-4 < x \le 0, \\ 0.08 & 0 < x \le 0.2\sin 2(2-\pi/2), \\ 0 & 0.2\sin 2(2-\pi/2) < x. \end{cases}$$

The comparison is given in Figures 3, 4 and 5.

We now compare with the direct method, in which one discretizes the δ function initial data and solves the Liouville equation directly. Using the the same discretized delta function (5.1) with the same parameter $b = 0.5\sqrt{dx}$, we compute the solution of this example by the direct method. The comparison of the results at time $t = 1$ and $t = 2$ is given in Figures 6 and 7, which shows that the decomposition method proposed in this paper gives a much more accurate solution especially for longer time.

Example 5.4. *(2d example) We consider a two-dimensional interface problem in the domain* $[-1,1]\times[-1,1]$. *The potential well is given by*

$$V = \begin{cases} 0 & x \in \Omega, \\ 1 & x \in \Omega^c. \end{cases} \qquad R = 0.2, \quad T = 0.8,$$

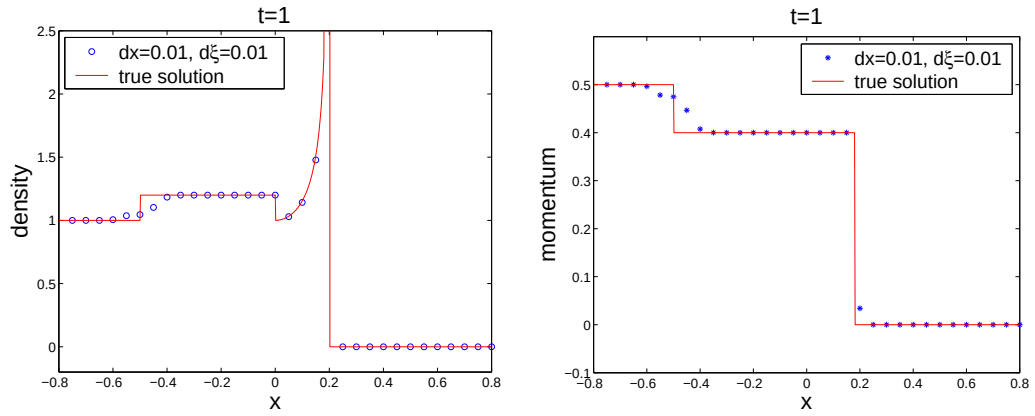

Figure 3: Example 5.3, the comparison of density and momentum between the reference solution and numerical solution at t=1.

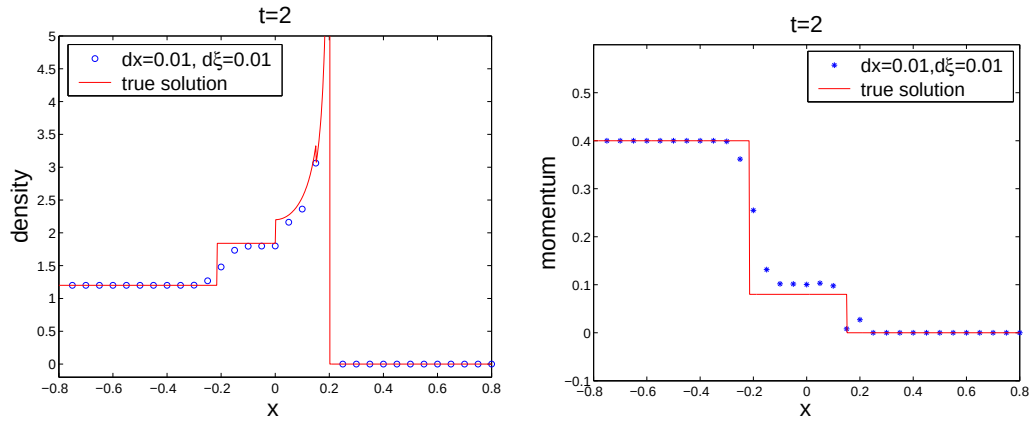

Figure 4: Example 5.3, the comparison of density and momentum between the reference solution and numerical solution at t=2, reinitialization was performed at t=1.

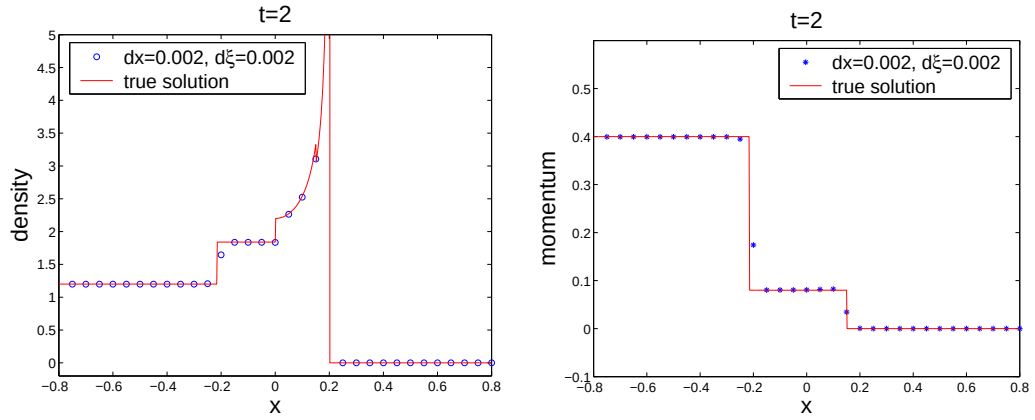

Figure 5: Example 5.3, the comparison of density and momentum between the reference solution and numerical solution at t=2 with a finer grid and $b = 0.15\sqrt{dx}$, reinitialization was performed at t=1.

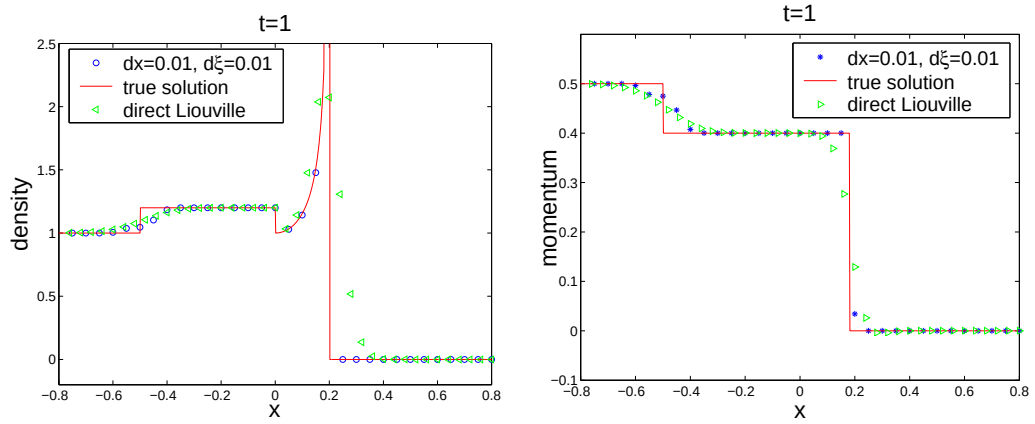

Figure 6: Example 5.3, the comparison of density and momentum between the solutions obtained by our method and by the direct method.

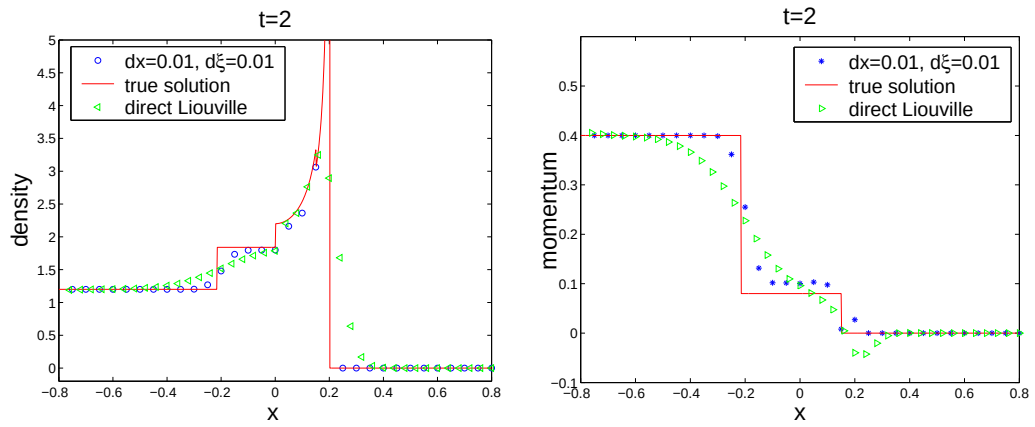

Figure 7: Example 5.3, the comparison of density and momentum between the solutions obtained by our method and by the direct method.

where $\Omega = \{(x,y)|\ y > -0.4,\ y - x - 0.5 < 0,\ y + x - 0.5 < 0\}$. *The initial condition is*

$$\rho_0(x,y) = I_{\{|x+0.5|<0.05,\ y>0.2\}}, \quad u_0 = (0, -\sqrt{2}).$$

See Figure 8 for the of the interface and the initial data.

We compare the numerical solution with analytical solution at $t = 1$. The analytical solution of the density at $t = 1$ can be obtained by the method of generalized characteristics, and it takes the following form:

$$\begin{aligned}\rho(x,y) \quad = \quad & I_{\text{reg}1}\delta(u - (0, -\sqrt{2})) + 0.2 I_{\text{reg}2}\delta(u - (-\sqrt{2}, 0)) + \frac{0.8}{\sqrt{3}} I_{\text{reg}3}\delta(u - (2\sin(\pi/12), -2\cos\pi/12)) \\ & + \frac{0.16}{\sqrt{3}} I_{\text{reg}4}\delta(u - (2\sin(\pi/12), 2\cos\pi/12) \\ & + \frac{1.28\cos(\pi/12)}{\sqrt{12\cos^2(\pi/12) - 6}} I_{\text{reg}5}\delta(u - (2\sin(\pi/12), -\sqrt{4\cos^2(\pi/12) - 2}),\end{aligned}$$

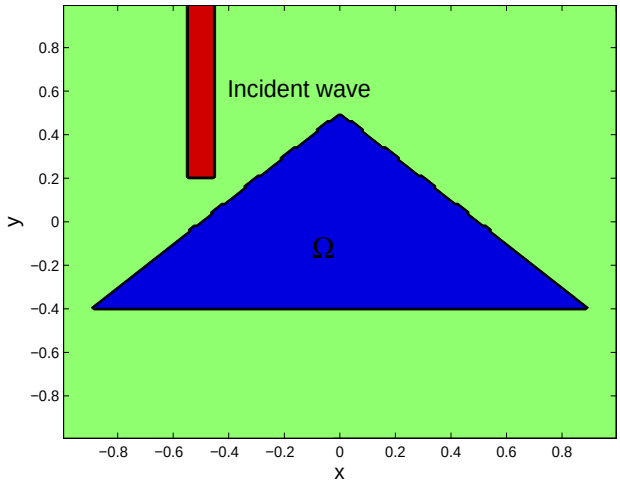

Figure 8: Illustration of the potential well and initial conditions in Example 5.4.

where

$$\begin{aligned}
\text{reg1} &= \{(x,y)|\ y-x-0.5>0,\ -0.55<x<-0.45.\},\\
\text{reg2} &= \{(x,y)|\ y-x-0.5>0,\ -0.05<y<0.05.\},\\
\text{reg3} &= \{(x,y)|\ y-x-0.5<0,\ y>-0.4,\ y<0.05-(x+0.45)/\tan(\pi/12),\\
&\qquad y>-0.05-(x+0.55)/\tan(\pi/12).\},\\
\text{reg4} &= \{(x,y)|\ y-x-0.5<0,\ y>-0.4,\ y>-0.4+(x-x_1)/\tan(\pi/12),\\
&\qquad y<-0.4+(x-x_2)/\tan(\pi/12).\},\\
\text{reg5} &= \{(x,y)|\ y-x-0.5<0,\ y<-0.4,\ y<-0.4-(x-x_1)\frac{\sqrt{4\cos^2(\pi/12)-2}}{2\sin(\pi/12)},\\
&\qquad y>-0.4-(x-x_2)\frac{\sqrt{4\cos^2(\pi/12)-2}}{2\sin(\pi/12)}.\},\\
x_1 &= 0.45\tan(\pi/12)-0.45,\quad x2=0.35\tan(\pi/12)-0.55.
\end{aligned}$$

The comparison of the numerical solution and the exact solution was shown in Figure 9, where the densities after the third transmission and reflection are ignored since their magnitudes are already very small. The mesh size is $dx = 0.000625,\ dy = 0.000625$ and the time step is taken to be $dt = 0.000125$.

Figure 10 gives a bird eye view of the solution.

Figure 11 gives a bird eye view of the solution with interface plotted. To better illustrate the result, the density in figure 11 was taken to be 2.5 times the original one.

6. Concluding remarks

References

[1] G. Bal, J.B. Keller, G. Papanicolaou and L. Ryzhik, Transport theory for acoustic waves with reflection and transmission at interfaces, Wave Motion, 30, 303-327 (1999).

[2] Li-Tien Cheng, Myungjoo Kang, Stanley Osher, Hyeseon Shim, and Yen-Hsi Tsai, Reflection in a Level Set Framework for Geometric Optics , Computer Modeling in Engineering and Sciences 5, 347-360, 2004.

[3] L.-T. Cheng, H.-L. Liu and S. Osher, Computational high-frequency wave propagation using the Level Set method, with applications to the semi-classical limit of Schrödinger equations, Comm. Math. Sci. 1, 593-621, 2003.

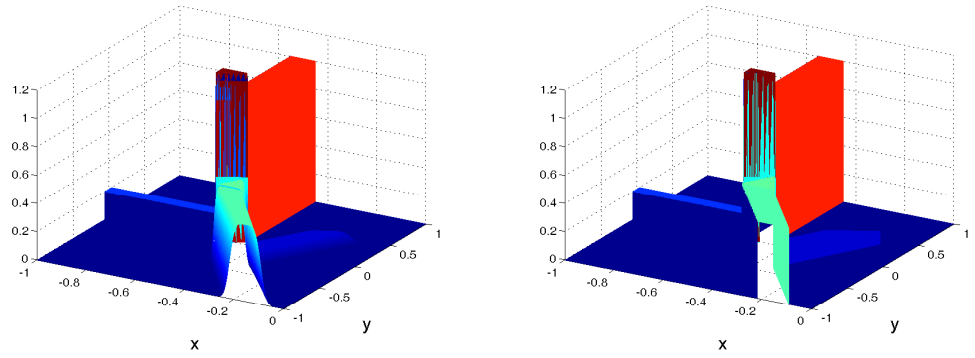

Figure 9: Example 5.4, the comparison of density between the numerical solution (left) and true solution (right) at t=1.

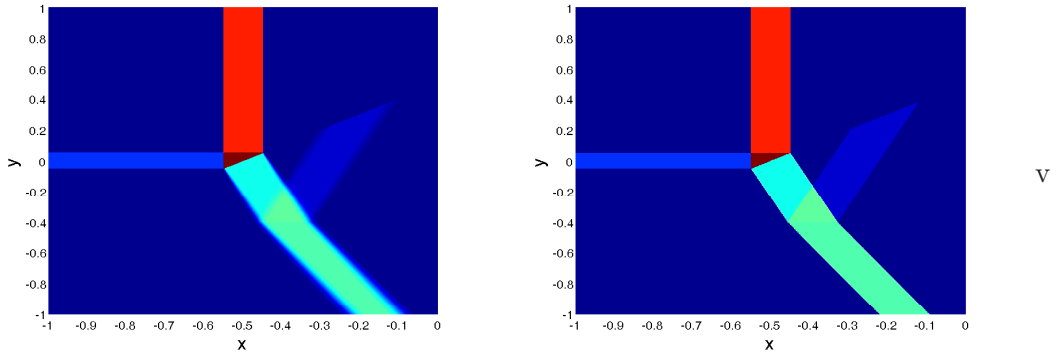

Figure 10: Example 5.4, a bird eye view of the density. Left: numerical solution. Right: true solution.

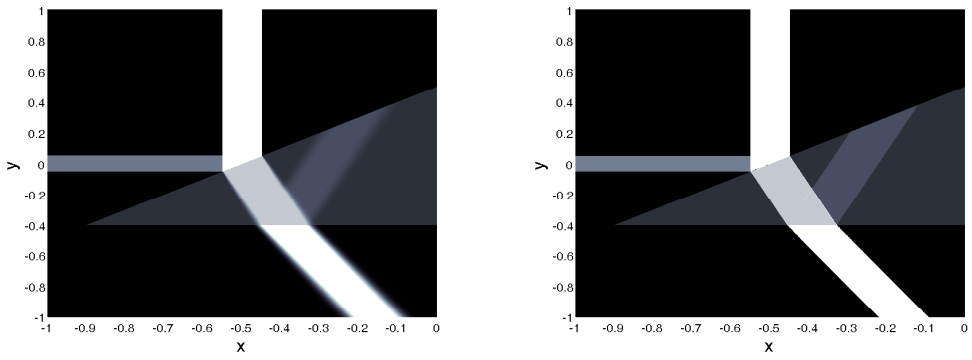

Figure 11: Example 5.4, a bird eye view of the density with interface plotted, to better illustrate the result, density was taken to be 2.5 times the original one. Left: numerical solution. Right: true solution.

[4] B. Engquist, A.K. Tornberg and R. Tsai, *Discretization of Dirac delta functions in level set methods*, J. Comput. Phys. 207 (2005), no. 1, 28–51.
[5] B. Engquist, O. Runborg and A.-K. Tornberg, High-Frequency Wave Propagation by the Segment Projection Method, J. Comput. Phys. 178(2), 373-390 (2002).
[6] S. Fomel and J.A. Sethian, Fast Phase Space Computation of Multiple Arrivals, Proc. Natl. Acad. Sci. USA 99(11), 7329-7334 (2002).
[7] P. Gerard, P.A. Markowich, N.J. Mauser, and F. Poupaud. Homogenization limits and Wigner transforms, Comm. Pure Appl. Math., 50(4), 323-379,1997.
[8] S. Jin and X.T. Li, Multi-phase Computations of the Semiclassical Limit of the Schrodinger Equation and Related Problems: Whitham vs. Wigner, Physica D 182, 46-85, 2003.
[9] S. Jin, H.L. Liu, S. Osher and R. Tsai, Computing multivalued physical observables for the semiclassical limit of the Schrodinger equation, J. Comp. Phys. 205, 222-241, 2005.
[10] S. Jin, H.L. Liu, S. Osher and R. Tsai, Computing multi-valued physical observables for high frequency limit of symmetric hyperbolic systems, J. Comp. Phys. 210, 497-518, 2005.
[11] S. Jin and K. Novak, A Semiclassical Transport Model for Thin Quantum Barriers, Multiscale Modeling and Simulation, 5(4), 1063-1086, 2006.
[12] S. Jin and K. Novak, A Semiclassical Transport Model for Two-Dimensional Thin Quantum Barriers, J. Comp. Phys. 226, 1623-1644, 2007.
[13] S. Jin and K. Novak, A coherent semiclassical transport model for pure-state quantum scattering, Comm. Math. Sci., to appear.
[14] S. Jin and S. Osher, A level set method for the computation of multi-valued solutions to quasi-linear hyperbolic PDE's and Hamilton-Jacobi equations, Comm. Math. Sci. 1(3), 575-591, 2003.
[15] S. Jin and X. Wen, Hamiltonian-preserving schemes for the Liouville equation with discontinuous potentials, Comm. Math. Sci. 3, 285-315, 2005.
[16] S. Jin and X. Wen, Hamiltonian-preserving schemes for the Liouville equation of geometrical optics with discontinuous local wave speeds, J. Comp. Phys., 214, 672-697, 2006.
[17] S. Jin and X. Wen, Hamiltonian-preserving schemes for the Liouville equation of geometrical optics with partial transmissions and reflections, SIAM J. Num. Anal. 44, 1801-1828, 2006.
[18] S. Jin and D. Yin, Computational high frequency waves through curved interfaces via the Loiuville equation and Geometric Theory of Diffraction, J. Comp. Phys. 227, 6106-6139, 2008.
[19] S. Jin and D. Yin, Computation of high frequency wave diffraction by a half plane via the Loiuville equation and Geometric Theory of Diffraction, Comm Comput Phys. 4, No. 5, 1106-1128, 2008.
[20] R.J. LeVeque, Numerical Methods for Conservation Laws, Birkhauser-Verlag, Basel, 1990.
[21] P.L. Lions and T. Paul, Sur les measures de Wigner, Revista. Mat. Iberoamericana 9, 1993, 553-618.
[22] L. Miller, Refraction of high frequency waves density by sharp interfaces and semiclassical measures at the boundary, J. Math. Pures Appl. IX 79, 227-269, (2000).
[23] S. Osher, L.-T. Cheng, M. Kang, H. Shim and Y.-H. Tsai, Geometric optics in a phase-space-based level set and Eulerian framework, J. Comput. Phys. 179(2), 622-648 (2002).
[24] L. Ryzhik, G. Papanicolaou and J. Keller, Transport equations for elastic and other waves in random media, Wave Motion 24, 327-370 DEC (1996).
[25] L. Ryzhik, G. Papanicolaou and J. Keller, Transport equations for waves in a half space, Comm. PDE's, 22, 1869-1910 (1997).
[26] C. Sparber, P. Markowich, N. Mauser, Multivalued geometrical optics: Wigner vs. WKB, Asymptotic Analysis 33, 1530187, 2003.
[27] D. Wei, *Weak solutions and critical thresholds for the one-dimensional Vlasov-Poisson equation*, preprint.

(Dongming Wei)
Department of Mathematics
University of Wisconsin
Madison, WI 53706 USA
E-mail address: dwei@math.wisc.edu

(Shi Jin)
Department of Mathematics
University of Wisconsin
Madison, WI 53706 USA
E-mail address: jin@math.wisc.edu

(Richard Tsai)
Department of Mathematics
University of Texas at Austin
Austin, TX 78712 USA
E-mail address: ytsai@math.utexas.edu

(Xu Yang)
Program in Applied and Computational Mathematics
Princeton University
Princeton, NJ 08544 USA
E-mail address: xuyang@math.princeton.edu